Hindawi Publishing Corporation
Mathematical Problems in Engineering
Volume 2013, Article ID 574696, 9 pages
http://dx.doi.org/10.1155/2013/574696

Research Article

Transient and Steady-State Responses of an Asymmetric Nonlinear Oscillator

Alex Elías-Zúñiga and Oscar Martínez-Romero

Departamento de Ingeniería Mecánica, Tecnológico de Monterrey, Campus Monterrey, E. Garza Sada 2501 Sur, 64849 Monterrey, NL, Mexico

Correspondence should be addressed to Alex Elías-Zúñiga; aelias@itesm.mx

Received 16 February 2013; Revised 4 May 2013; Accepted 10 May 2013

Academic Editor: Miguel A. F. Sanjuán

We study the dynamical response of an asymmetric forced, damped Helmholtz-Duffing oscillator by using Jacobi elliptic functions, the method of elliptic balance, and Fourier series. By assuming that the modulus of the elliptic functions is slowly varying as a function of time and by considering the primary resonance response of the Helmholtz-Duffing oscillator, we derived an approximate solution that provides the time-dependent amplitude-frequency response curves. The accuracy of the derived approximate solution is evaluated by studying the evolution of the response curves of an asymmetric Duffing oscillator that describes the motion of a damped, forced system supported symmetrically by simple shear springs on a smooth inclined bearing surface. We also use the percentage overshoot value to study the influence of damping and nonlinearity on the transient and steady-state oscillatory amplitudes.

1. Introduction

Since most of the nonlinear differential equations that characterized the motion of several physical systems do not have closed-form solution, we have to use numerical or perturbation techniques to study the dynamical response of these systems. However, most of the perturbation techniques such as multiple scales, averaging, and harmonic balance, to say a few, focus on only the determination of steady-state approximate solutions because of the complexity involved in finding transient solutions of nonlinear differential equations [1, 2].

The aim of this paper is to investigate the influence on the dynamical behavior of the transient and steady-state solutions of the system

$$\ddot{x} + 2\nu\dot{x} + Ax + Bx^2 + \varepsilon x^3 = F\cos\left(\omega_f t\right) \tag{1}$$

close to the primary resonance region. Here, x denotes the displacement of the system, A is the natural frequency, ν is the damping coefficient, ε is a dimensionless nonlinear parameter, ω_f is the driving frequency, t is the running time, F is the amplitude of the driving force, and B is a system parameter. To solve the homogeneous Helmholtz-Duffing oscillator for which $F = 0$ in (1), Hu used the harmonic balance method to calculate the first-order approximations to the periodic solutions of this equation [3]. Belhaq and Lakrad used the harmonic balance method involving Jacobian elliptic functions to obtain the approximate solution of (1) by taking $\nu = 0$ and $\omega_f = 0$ [4]. Tamura [5] and Hu [6] developed the exact solution of a quadratic nonlinear oscillator that is part of (1) by using an elliptic function. Cao and coworkers investigated in [7] the various symmetry breaking phenomena associated with the Helmholtz-Duffing oscillator (1) in the case for which $B = 1 - \varepsilon$ and for different values of the so-called symmetric parameter ε. They also used the second-order averaging method to investigate its local bifurcation behavior. By considering a rational form elliptic solution to (1) when $F = 0$, Elías-Zúñiga derived its analytical solution which is similar in form to that of its exact solution when $\nu = 0$ [8].

Recently, Kovacic and coworkers studied the primary resonance response of (1) by applying the harmonic balance method and derived nonlinear algebraic equations for

the steady-state system response [9], while Jeyakumari et al. analyzed how the potential well of an asymmetric Duffing oscillator affects the vibrational resonance response [10].

Here the approximate solution of (1) is derived by taking into account the transient and the steady-state responses without the simplifications regarding undamped and unforced system included in previously developed solutions such as [4, 6]. The approximate solution is based on trigonometric and Jacobi elliptic functions with slowly varying parameters that will help us to obtain amplitude-frequency response curves that evolve with time. Then, the influence of the nonlinear transient responses is investigated since recent studies show that transient vibrations can not only provide additional information to fully predict the system stable behavior [11], but also can be used to predict the system overshoot value [12, 13]. The determination of this value is of practical interest in understanding the importance of time in controlling the dynamical behavior of oscillatory systems [14, 15] therefore, the percentage overshoot value will be computed by considering the influence of the system parameters such as nonlinear and damping effects.

In the next section, the approximate general solution of (1) is derived by using Jacobi elliptic functions.

2. Approximate Solution

In order to obtain the general solution of (1) in the region of the primary resonance, we will consider that this equation can be written in equivalent form as

$$\ddot{x} + 2\nu\dot{x} + Ax + Bx^2 + \varepsilon x^3 = F\mathrm{cn}\left(\omega_f t, k_f^2\right), \tag{2}$$

where $\mathrm{cn}(\omega_f t, k_f^2)$ is the Jacobian elliptic function that has a period in $\omega_f t$ equal to $4K(k_f^2)$, and $K(k_f^2)$ is the complete elliptic integral of the first kind for the modulus k_f [16, 17]. Note that $0 \le |k_f^2| < 1$ must hold, and when the modulus of $\mathrm{cn}(\omega_f t, k_f^2)$ is zero, then $\mathrm{cn}(\omega_f t, k_f^2)$ and the trigonometric function $\cos(\omega_f t)$ coincide and, thus, (2) reduces to (1). Now, we make the assumption that (2) has an approximate general solution of the form

$$\begin{aligned} x = {} & b(t) + c(t)\,\mathrm{cn}\left(\omega_1 t + \phi_1, k_1^2\right) + D_1(t)\,\mathrm{cn}\left(\omega_f t, k_f^2\right) \\ & + D_2(t)\,\mathrm{sn}\left(\omega_f t, k_f^2\right), \end{aligned} \tag{3}$$

where ϕ_1, $\omega_1(t)$, $b(t)$, $D_1(t)$, $D_2(t)$, $k_1(t)$, and $k_f(t)$ need to be determined. For the sake of simplicity, it is assumed that $b(t)$, $\omega_1(t)$, $D_1(t)$, $D_2(t)$, $k_1(t)$, and $k_f(t)$ are slowly varying as a function of time so that $\dot{b}$, $\dot{\omega}_1$, $\dot{D}_1$, $\dot{D}_2$, $\dot{k}_1$, and $\dot{k}_f$ or higher order are small enough to be ignored [18]. Also, for simplicity, we will use the following notation $\mathrm{cn}_f \equiv \mathrm{cn}u_f = \mathrm{cn}(\omega_f t, k_f^2)$, and $\mathrm{cn}_1 \equiv \mathrm{cn}u_1 = \mathrm{cn}(\omega_1 t + \phi_1, k_1^2)$ with similar notation for the functions sn and dn. Thus, substitution of (3) into (2) gives

$$\begin{aligned} & Ab + b^2 B + b^3\varepsilon \\ & + \mathrm{cn}_1\left[Ac + 2bBc + 3b^2\varepsilon c \right. \\ & \qquad + \mathrm{cn}_f\left(2BcD_1 + 6b\varepsilon cD_1\right) + 3\varepsilon cD_1^2\mathrm{cn}_f^2 \\ & \qquad - \omega_1^2 c + 2k_1^2\omega_1^2 c + \mathrm{sn}_f\left(2BcD_2 + 6b\varepsilon cD_2\right) \\ & \qquad \left. + 3\varepsilon cD_2^2\mathrm{sn}_f^2 + 2\nu\dot{c} + \ddot{c}\right] \\ & + \mathrm{cn}_1^2\left[Bc^2 + 3b\varepsilon c^2\right] + \mathrm{cn}_1^3\left[\varepsilon c^3 - 2\omega_1^2 k_1^2 c\right] \\ & - 2\omega_1\mathrm{dn}_1\mathrm{sn}_1\left[\nu c + \dot{c}\right] + \mathrm{cn}_f\mathrm{dn}_f\left[2\nu\omega_f D_2\right] \\ & + \mathrm{cn}_f\left[-F + AD_1 + 2bBD_1 + 3b^2\varepsilon D_1 \right. \\ & \qquad + 3\varepsilon c^2 D_1\mathrm{cn}_1^2 + 2\omega_f^2 k_f^2 D_1 - \omega_f^2 D_1 \\ & \qquad \left. + \mathrm{sn}_f\left(2BD_1D_2 + 6b\varepsilon D_1D_2\right) + 3\varepsilon D_1D_2^2\mathrm{sn}_f^2\right] \\ & + \mathrm{cn}_f^2\left[BD_1^2 + 3b\varepsilon D_1^2\right] + \mathrm{cn}_f^3\left[\varepsilon D_1^3 - 2\omega_f^2 k_f^2 D_1\right] \\ & - \mathrm{dn}_f\mathrm{sn}_f\left[2\nu\omega_f D_1\right] + \mathrm{cn}_1\mathrm{cn}_f\mathrm{sn}_f\left[6\varepsilon cD_1D_2\right] \\ & + \mathrm{sn}_f\left[AD_2 + 2bBD_2 + 3b^2\varepsilon D_2 + 3\varepsilon c^2 D_2\mathrm{cn}_1^2 \right. \\ & \qquad \left. + 3\varepsilon D_1^2 D_2\mathrm{cn}_f^2 - k_f^2\omega_f^2 D_2 - \omega_f^2 D_2\right] \\ & + \mathrm{sn}_f^2\left[BD_2^2 + 3b\varepsilon D_2^2\right] \\ & + \mathrm{sn}_f^3\left[\varepsilon D_2^3 + 2\omega_f^2 k_f^2 D_2\right] = 0 \end{aligned} \tag{4}$$

in which the following identities $\mathrm{sn}^2 + \mathrm{cn}^2 = 1$ and $\mathrm{dn}^2 + k_j^2\mathrm{sn}^2 = 1$ have been used [19].

Notice that (4) depends on elliptic functions with different modulus. To simplify (4), we first compute its average with respect to $4K_f$ while keeping terms with period $4K_1$ constant; this yields the following equation:

$$\begin{aligned} & Ab + b^2 B + b^3\varepsilon + \left(1 - I_f\right)\left[BD_2^2 + 3b\varepsilon D_2^2\right] \\ & \quad + I_f\left[BD_1^2 + 3b\varepsilon D_1^2\right] \\ & \quad + \mathrm{cn}_1\left[Ac + 2bBc + 3b^2\varepsilon c + 3\varepsilon cD_1^2 I_f - \omega_1^2 c \right. \\ & \qquad \left. + 2k_1^2\omega_1^2 c + 3\varepsilon cD_2^2\left(1 - I_f\right) + 2\nu\dot{c} + \ddot{c}\right] \\ & \quad + \mathrm{cn}_1^2\left[Bc^2 + 3b\varepsilon c^2\right] - 2\omega_1\mathrm{dn}_1\mathrm{sn}_1\left[\nu c + \dot{c}\right] \\ & \quad + \mathrm{cn}_1^3\left[\varepsilon c^3 - 2\omega_1^2 k_1^2 c\right] = 0. \end{aligned} \tag{5}$$

We now take the average of (5) with respect to $4K_1$, to get

$$\begin{aligned} &Ab + b^2B + b^3\varepsilon + \left(1 - I_f\right)\left[BD_2^2 + 3b\varepsilon D_2^2\right] \\ &\quad + I_f\left[BD_1^2 + 3b\varepsilon D_1^2\right] + I_1c^2\left(B + 3b\varepsilon\right) = 0, \end{aligned} \tag{6}$$

where the I_j terms are defined in the appendix.

Next, the average of (4) is computed with respect to $4K_1$ while terms with period $4K_f$ are held constant; this yields

$$\begin{aligned} &Ab + b^2B + b^3\varepsilon + I_1\left[Bc^2 + 3b\varepsilon c^2\right] \\ &\quad + \mathrm{cn}_f\mathrm{sn}_f\left(2BD_1D_2 + 6b\varepsilon D_1D_2\right) \\ &\quad \times \mathrm{cn}_f\left[-F + AD_1 + 2bBD_1 + 3b^2\varepsilon D_1 + 3\varepsilon c^2D_1I_1\right. \\ &\qquad \left. + 2\omega_f^2k_f^2D_1 - \omega_f^2D_1 + 3\varepsilon D_1D_2^2\right] \\ &\quad + \mathrm{cn}_f^2\left[BD_1^2 + 3b\varepsilon D_1^2\right] \\ &\quad + \mathrm{cn}_f^3\left[\varepsilon D_1^3 - 2\omega_f^2k_f^2D_1 - 3\varepsilon D_1D_2^2\right] \\ &\quad + \mathrm{cn}_f\mathrm{dn}_f\left[2\nu\omega_fD_2\right] - \mathrm{dn}_f\mathrm{sn}_f\left[2\nu\omega_fD_1\right] \\ &\quad + \mathrm{sn}_f^2\left[BD_2^2 + 3b\varepsilon D_2^2\right] \\ &\quad + \mathrm{sn}_f\left[AD_2 + 2bBD_2 + 3b^2\varepsilon D_2\right. \\ &\qquad \left. + 3\varepsilon c^2D_2I_1 + k_f^2\omega_f^2D_2 - \omega_f^2D_2 + \varepsilon D_2^3\right] \\ &\quad - \mathrm{sn}_f\mathrm{cn}_f^2\left[\varepsilon D_2^3 + 2\omega_f^2k_f^2D_2 - 3\varepsilon D_1^2D_2\right] = 0. \end{aligned} \tag{7}$$

Then, the average of (7) is computed with respect to $4K_f$, to get the following expression:

$$\begin{aligned} &Ab + b^2B + b^3\varepsilon + I_f\left[BD_1^2 + 3b\varepsilon D_1^2 - BD_2^2 - 3b\varepsilon D_2^2\right] \\ &\quad + I_1\left[Bc^2 + 3b\varepsilon c^2\right] + \left(BD_2^2 + 3b\varepsilon D_2^2\right) = 0. \end{aligned} \tag{8}$$

To determine the unknown parameters ϕ_1, $\omega_1(t)$, $b(t)$, $D_1(t)$, $D_2(t)$, $k_1(t)$, and $k_f(t)$, Fourier series are applied to (7) to transform the terms sn dn and sn cn^2 into sn, cn sn and cn dn into cn Jacobian elliptic functions, respectively [20–22]. Therefore, (7) simplifies to

$$\begin{aligned} &\mathrm{cn}_f\left[-F + AD_1 + 2bBD_1 + 3b^2\varepsilon D_1 + 3\varepsilon c^2D_1I_1\right. \\ &\qquad \left. + 2\omega_f^2k_f^2D_1 - \omega_f^2D_1 + 3\varepsilon D_1D_2^2 + 2\nu\omega_fD_2H_2\right] \\ &\quad + \mathrm{cn}_f^2\left[BD_1^2 + 3b\varepsilon D_1^2\right] \\ &\quad + \mathrm{cn}_f^3\left[\varepsilon D_1^3 - 2\omega_f^2k_f^2D_1 - 3\varepsilon D_1D_2^2\right] \\ &\quad + \mathrm{sn}_f^2\left[BD_2^2 + 3b\varepsilon D_2^2\right] \\ &\quad + \mathrm{sn}_f\left[AD_2 + 2bBD_2 + 3b^2\varepsilon D_2 + 3\varepsilon c^2D_2I_1\right. \\ &\qquad + k_f^2\omega_f^2D_2 - \omega_f^2D_2 + \varepsilon D_2^3 - 2\nu\omega_fD_1H_1 \\ &\qquad \left. - \left(\varepsilon D_2^3 + 2\omega_f^2k_f^2D_2 - 3\varepsilon D_1^2D_2\right)H_3\right] \\ &\quad + Ab + b^2B + b^3\varepsilon + I_1\left[Bc^2 + 3b\varepsilon c^2\right] \\ &\quad + \left(\text{higher harmonics}\right) = 0, \end{aligned} \tag{9}$$

where H_1, H_2, and H_3 are defined in the appendix. If we now use the amplitude for Jacobi elliptic functions so that $\cos\varphi_j = \mathrm{cn}(\omega_jt; k_j^2) = \mathrm{cn}_j$, and $\sin\varphi_j = \mathrm{sn}(\omega_jt; k_j^2) = \mathrm{sn}_j$, then (5) and (9) become

$$\begin{aligned} &Ab + b^2B + b^3\varepsilon + \left(1 - I_f\right)\left[BD_2^2 + 3b\varepsilon D_2^2\right] \\ &\quad + I_f\left[BD_1^2 + 3b\varepsilon D_1^2\right] \\ &\quad + \cos\varphi_1\left[Ac + 2bBc + 3b^2\varepsilon c + 3\varepsilon cD_1^2I_f - \omega_1^2c\right. \\ &\qquad \left. + 2k_1^2\omega_1^2c + 3\varepsilon cD_2^2\left(1 - I_f\right) + 2\nu\dot{c} + \ddot{c}\right] \\ &\quad + \cos^2\varphi_1\left[Bc^2 + 3b\varepsilon c^2\right] \\ &\quad - 2\omega_1\sqrt{1 - k_1^2\sin\varphi_1^2}\sin\varphi_1\left[\nu c + \dot{c}\right] \\ &\quad + \cos^3\varphi_1\left[\varepsilon c^3 - 2\omega_1^2k_1^2c\right] = 0, \\ &\cos\varphi_f\left[-F + AD_1 + 2bBD_1 + 3b^2\varepsilon D_1\right. \\ &\qquad + 3\varepsilon c^2D_1I_1 + 2\omega_f^2k_f^2D_1 - \omega_f^2D_1 \\ &\qquad + 3\varepsilon D_1D_2^2 + 2\nu\omega_fD_2H_2 \\ &\qquad \left. + \frac{3}{4}\left(\varepsilon D_1^3 - 2\omega_f^2k_f^2D_1 - 3\varepsilon D_1D_2^2\right)\right] \\ &\quad + \sin\varphi_f\left[AD_2 + 2bBD_2 + 3b^2\varepsilon D_2 + 3\varepsilon c^2D_2I_1\right. \\ &\qquad + k_f^2\omega_f^2D_2 - \omega_f^2D_2 + \varepsilon D_2^3 - 2\nu\omega_fD_1H_1 \\ &\qquad \left. - \left(\varepsilon D_2^3 + 2\omega_f^2k_f^2D_2 - 3\varepsilon D_1^2D_2\right)H_3\right] \\ &\quad + \left[Ab + b^2B + b^3\varepsilon\right. \\ &\qquad \left. + I_1\left[Bc^2 + 3b\varepsilon c^2\right] + \frac{1}{2}\left(BD_1^2 + 3b\varepsilon D_1^2 + BD_2^2 + 3b\varepsilon D_2^2\right)\right] \\ &\quad + \left(\text{higher harmonics}\right) = 0. \end{aligned} \tag{10}$$

Since our original system (1) is subjected to a driving force of sinusoidal type, then the modulus $k_f \equiv 0$ and the following identities hold: $\mathrm{cn}_f = \cos_f$, $\mathrm{sn}_f = \sin_f$, $I_f = 1/2$, $H_1 = 1$,

and $H_2 = 1$. If we also assume that $0 < |k_1^2| < 1/2$, then, from (A.1), $I_1 \simeq 1/2$ and (6) becomes exactly the same as (8). This provides the following simplifications for (10):

$$\begin{aligned}
&\cos\varphi_1 \left[Ac + \frac{3}{4}\left(\varepsilon c^3 - 2\omega_1^2 k_1^2 c\right) + 2bBc \right.\\
&\qquad + 3b^2\varepsilon c + \frac{3}{2}\varepsilon c\left(D_1^2 + D_2^2\right) - \omega_1^2 c\\
&\qquad \left. + 2k_1^2\omega_1^2 c + 2\nu\dot{c} + \ddot{c}\right] - 2\omega_1 \sin\varphi_1 \left[\nu c + \dot{c}\right]\\
&+ \frac{1}{4}\cos 3\varphi_1 \left[\varepsilon c^3 - 2\omega_1^2 k_1^2 c\right]\\
&+ (\text{higher harmonics}) = 0,\\
&\cos_f \left[-F + AD_1 + 2bBD_1 + 3b^2\varepsilon D_1 + \frac{3}{2}\varepsilon c^2 D_1 \right.\\
&\qquad - \omega_f^2 D_1 + 3\varepsilon D_1 D_2^2 + 2\nu\omega_f D_2\\
&\qquad \left. + \frac{3}{4}\left(\varepsilon D_1^3 - 3\varepsilon D_1 D_2^2\right)\right]\\
&+ \sin_f \left[AD_2 + 2bBD_2 + 3b^2\varepsilon D_2 \right.\\
&\qquad + \frac{3}{2}\varepsilon c^2 D_2 - \omega_f^2 D_2 + \varepsilon D_2^3\\
&\qquad \left. - 2\nu\omega_f D_1 - \frac{1}{4}\left(\varepsilon D_2^3 - 3\varepsilon D_1^2 D_2\right)\right]\\
&+ (\text{higher harmonics}) = 0.
\end{aligned} \tag{11}$$

We then follow the harmonic balance procedure and ignore higher harmonics terms in (11), to find the following expressions:

$$\begin{aligned}
&Ac + \frac{3}{4}\left(\varepsilon c^3 - 2\omega_1^2 k_1^2 c\right) + 2bBc + 3b^2\varepsilon c\\
&+ \frac{3}{2}\varepsilon c\left(D_1^2 + D_2^2\right) - \omega_1^2 c + 2k_1^2\omega_1^2 c + 2\nu\dot{c} + \ddot{c} = 0,
\end{aligned} \tag{12}$$

$$\begin{aligned}
&-F + AD_1 + 2bBD_1 + 3b^2\varepsilon D_1 + \frac{3}{2}\varepsilon c^2 D_1 - \omega_f^2 D_1\\
&+ \frac{3}{4}\varepsilon D_1 D_2^2 + 2\nu\omega_f D_2 + \frac{3}{4}\varepsilon D_1^3 = 0,
\end{aligned} \tag{13}$$

$$\begin{aligned}
&AD_2 + 2bBD_2 + 3b^2\varepsilon D_2 + \frac{3}{2}\varepsilon c^2 D_2 - \omega_f^2 D_2\\
&+ \frac{3}{4}\varepsilon D_2^3 - 2\nu\omega_f D_1 + \frac{3}{4}\varepsilon D_1^2 D_2 = 0,
\end{aligned} \tag{14}$$

$$\varepsilon c^3 - 2\omega_1^2 k_1^2 c = 0, \tag{15}$$

$$\nu c + \dot{c} = 0. \tag{16}$$

Notice that the variable c may be determined by integration of (16); this yields

$$c(t) = C\exp(-\nu t), \tag{17}$$

where C is a constant of integration. Substitution of (17) into (8), as well as (12)–(15), yields

$$\begin{aligned}
-\frac{D_2^2}{2}(B + 3b\varepsilon) &= Ab + b^2 B + b^3\varepsilon\\
&+ \frac{1}{2}C^2\exp(-2\nu t)(B + 3b\varepsilon)\\
&+ \frac{D_1^2}{2}(B + 3b\varepsilon),
\end{aligned} \tag{18}$$

$$\begin{aligned}
\omega_1^2 &= A + 2bB + 3b^2\varepsilon + \frac{3}{2}\varepsilon\left(D_1^2 + D_2^2\right)\\
&+ \varepsilon C^2\exp(-2\nu t) - \frac{\nu^2}{4},
\end{aligned} \tag{19}$$

$$\begin{aligned}
-\frac{3}{4}\varepsilon\left(D_1^2 + D_2^2\right) &= -\frac{F}{D_1} + A + 2bB + 3b^2\varepsilon\\
&+ 2\nu\omega_f\frac{D_2}{D_1} + \frac{3}{2}\varepsilon C^2\exp(-2\nu t)\\
&- \omega_f^2,
\end{aligned} \tag{20}$$

$$\begin{aligned}
-\frac{3}{4}\varepsilon\left(D_1^2 + D_2^2\right) &= A + 2bB + 3b^2\varepsilon\\
&+ \frac{3}{2}\varepsilon C^2\exp(-2\nu t) - \omega_f^2\\
&- 2\nu\omega_f\frac{D_1}{D_2},
\end{aligned} \tag{21}$$

$$k_1^2 = \frac{\varepsilon C^2\exp(-2\nu t)}{2\omega_1^2}. \tag{22}$$

Then, for given parameters values of ν, ε, A, B, F, and ω_f, the unknown parameters ϕ_1, ω_1, C, D_1, D_2, b, and k_1 can be found from (18)–(22) and from the initial conditions (I. C.) $x(0) = x_{10}$, $\dot{x}(0) = \dot{x}_{10}$. If we assume that the value of the initial velocity $\dot{x}(0) = \dot{x}_{10}$ is such that $\phi_1 = 0$ in (3), then our approximate solution for (2) can be written as

$$\begin{aligned}
x &= b(t) + C\exp(-\nu t)\,\mathrm{cn}\left(\omega_1 t, k_1^2\right)\\
&+ D_1(t)\cos\left(\omega_f t\right) + D_2(t)\sin\left(\omega_f t\right).
\end{aligned} \tag{23}$$

Since $x(0) = x_{10}$ at $t = 0$, we get from (23) that

$$C = x_{10} - b(0) - D_1(0). \tag{24}$$

We next use (20) and (21) to find $b(t)$ and $D_2(t)$ as

$$D_2(t) = \frac{F \mp \sqrt{F^2 - \left(4\nu\omega_f D_1\right)^2}}{4\nu\omega_f}, \tag{25}$$

$$b(t) = \frac{1}{384 D_1 \varepsilon \nu^2 \omega_f^2} \times \Big(-128 B D_1 \nu^2 \omega_f^2 \mp \Big[256 D_1 \nu^2 \omega_f^2 \times \Big(64 B^2 D_1 \nu^2 \omega_f^2 + 3\varepsilon \times \Big(32 \nu^2 \omega_f^2 (F \pm R_1) \times -D_1 \Big(6\varepsilon F^2 \mp 6\varepsilon F R_1 + 32 \nu^2 \omega_f^2 \times \Big(2A + 3C^2 \exp(-2\nu t)\,\varepsilon - 2\omega_f^2\Big)\Big)\Big)\Big)\Big]^{1/2}\Big), \tag{26}$$

$$R_1 = \sqrt{\big(F - 4 D_1 \nu \omega_f\big)\big(F + 4 D_1 \nu \omega_f\big)}, \tag{27}$$

where the sign in (25) and (26) must be appropriately chosen to ensure that the higher elliptic terms in (23) have small amplitudes relative to the leading ones [23]. Substituting (25) and (26) into (18), we can easily prove, after some algebraic computations, that the values of $D_1(t)$ are determined from a ninth-order polynomial equation. Once the values of $D_1(t)$ are known, we may use (19) to determine $\omega_1(t)$. Notice that when the running time t increases, the term $e^{-\nu t}$ approaches to zero, and thus (18), (19), and (22)–(26) become time-independent. In this case, the values of b, D_1, D_2, ω_1, and k_1 in (23) will remain constant. This condition provides the steady-state solution of (1).

We will next discuss the accuracy of our derived approximate solution by studying the dynamical response of an asymmetric Duffing oscillator by plotting the amplitude-frequency and the percentage overshoot response curves and show how the evolution of time influences the systems behavior.

3. Numerical Simulations

In order to verify the accuracy of our proposed solution described in (23), we study the dynamical response of a rigid body supported symmetrically by a simple shear spring that is sliding over a smooth inclined bearing surface [24]. The system under consideration contains the following critical conditions: (a) finite amplitude forced vibration and (b) damping, demonstrating the general nature of the proposed solution for the resonance response of an asymmetric Duffing oscillator. In accordance with Elías-Zúñiga and Beatty [24], the equation for the damped motion of the load is a nonlinear, ordinary differential equation of the forced Duffing type with a constant static shift term of the form

$$\ddot{\sigma} + 2\nu\dot{\sigma} + \sigma + \varepsilon\sigma^3 = \sigma_e\left(1 + \varepsilon\sigma_e^2\right) + F\cos\omega_f t, \tag{28}$$

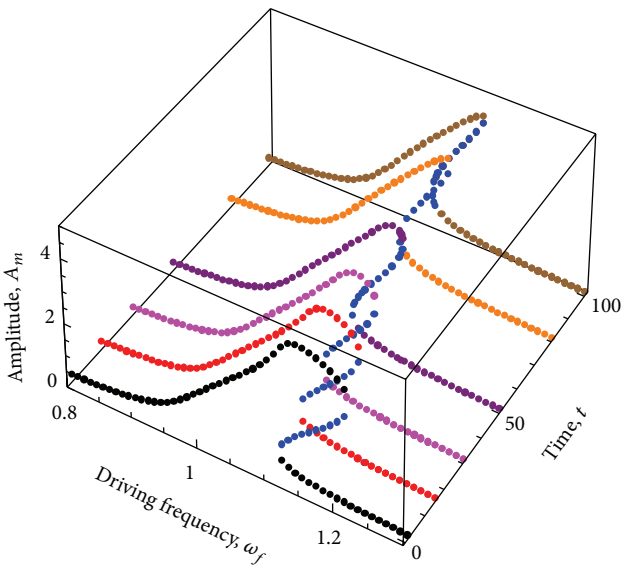

Figure 1: Evolutive amplitude-frequency response curves of a rigid body supported symmetrically by a simple shear spring and sliding over a smooth inclined bearing surface with moderate static shear deflection $\sigma_e = 0.497$ and parameter values of $\varepsilon = 0.02$, $F = 0.1$, $\nu = 0.01$, and initial conditions $x_0 = 1$ and $\dot{x}_0 = -0.0091$. At $t = 0$, the initial values of b, C, D_1, D_2, k_1, and ω_1 are given as $b(0) = -0.0121$, $C = 0.9951$, $D_1(0) = 0.0962$, $D_2(0) = 0$, $k_1(0) = 0.0902$, and $\omega_1(0) = 1.0154$. The blue dot curves represent unstable system response.

where the dot denotes the derivative with respect to t, σ represents the amount of simple shear deformation, σ_e denotes the amount of static shear deflection of the load, ν is the damping ratio, F is a dimensionless driving force, and t is the dimensionless running time. If we transform (28) relative to σ_e by using $x = \sigma - \sigma_e$, then (28) becomes similar to the Helmholtz-Duffing equation (1) where the parameters A and B are described by

$$A \equiv 1 + 3\varepsilon\sigma_e^2, \qquad B \equiv 3\varepsilon\sigma_e. \tag{29}$$

To find the amplitude-frequency response curves of (1), we select the following parameter values: $\varepsilon = 0.02$, $\sigma_e = 0.497$, $F = 0.1$, $\nu = 0.01$, $x_0 = 1$, and $\dot{x}_0 = 0.022$, and plot these curves at the values of $t = 1$, 15, 30, 80, and 100. Figure 1 shows the evolution of these amplitude-frequency curves with time. In the curves showed in Figure 1, we have plotted $A_m(t) = |b(t) + D_1(t) + D_2(t)|$ versus ω_f. These curves characterize the evolution of the general motion of the system for the selected set of system parameter values. In these curves, the blue dots represent unstable system behavior determined by following the bifurcation analysis described in [9, 24]. Notice from Figure 1, that when the running time t increases, that is, $t \approx 100$, the unstable regions in the amplitude-frequency response curves become smaller since the influence of time in (18), (19), and (22)–(26) is almost negligible. In Figure 1, the brown dots represent the stable steady-state amplitude-frequency response curve that characterizes the damped, forced nonlinear motion of a body supported by viscohyperelastic shear mountings [24].

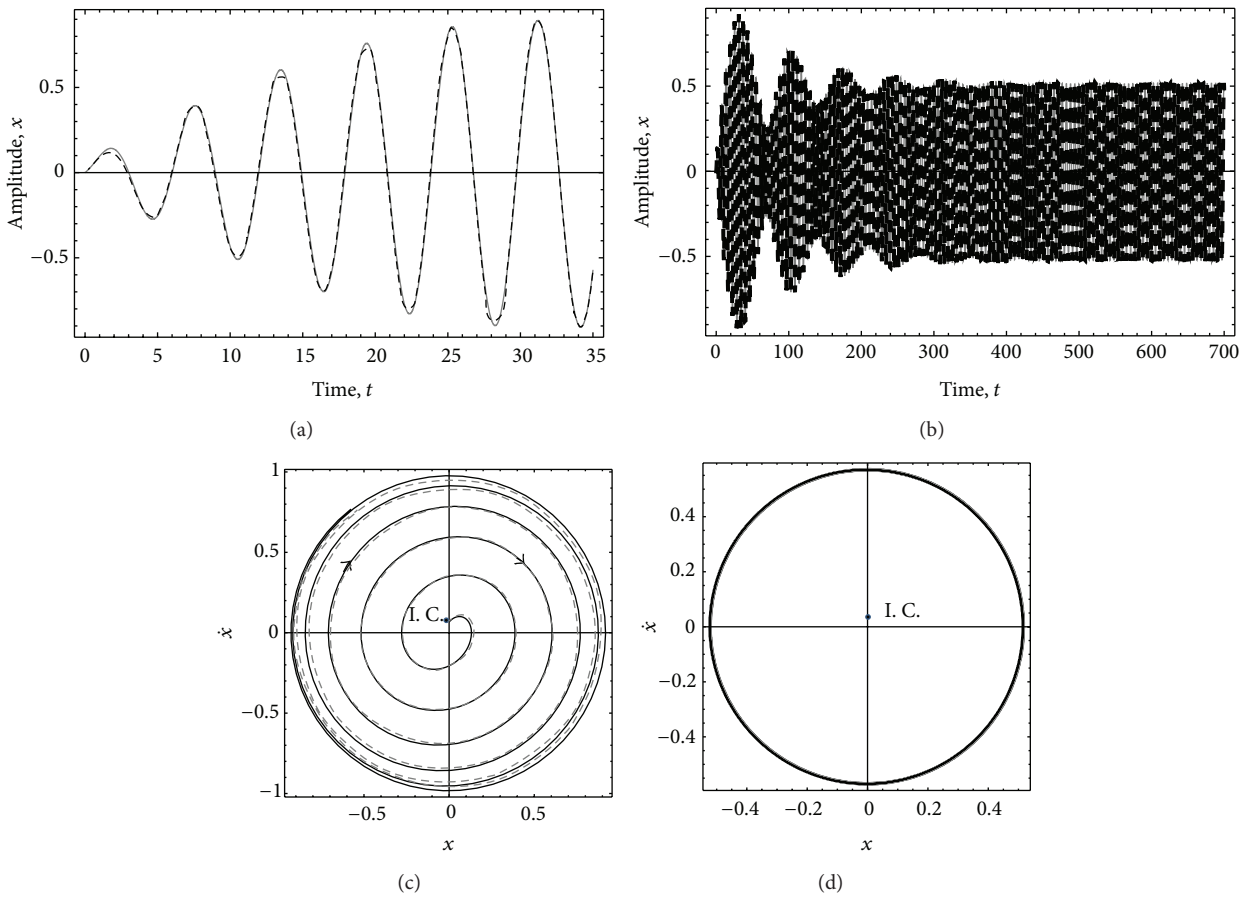

FIGURE 2: Phase portraits and amplitude-time response curves for parameter values of $\varepsilon = 0.02$, $\sigma_e = 0.497$, $\nu = 0.01$, $F = 0.1$, $\omega_f = 1.1$, $D_1(0) = -0.541$, $D_2(0) = 0.0653$, $b(0) = -0.0086$, $k_1(0) = 0.05418$, $\omega_1(0) = 1.0144$, $C = 0.5496$, and initial conditions $x(0) = 0$ and $\dot{x}(0) = 0.0663$. (a) Amplitude-time transient curves on $t[0, 31.5]$; (b) amplitude-time response curve on $t[0, 700]$; (c) transient response phase portrait; (d) steady-state system response phase portrait on $t[650, 700]$. The solid lines represent the numerical solution, and the dashed lines represent the proposed EBM solution.

Figure 2 illustrates the amplitude versus time response curve by considering the parameters values of $\sigma_e = 0.497$, $\varepsilon = 0.02$, $\nu = 0.01$, $F = 0.1$, and $\omega_f = 1.1$ and the initial conditions $x_0 = 0$ and $\dot{x}_0 = 0.0663$ for which $\phi_1 = 0$. There, the solid lines represent the numerical integration solution of (28) while the dashed lines represent the approximate solution provided by (23). In this case, the values of b, C, D_1, D_2, k_1, and ω_1 were obtained from (18), (19), (22), (24), (25), and (26). In fact, at $t = 0$, we get that $b(0) = -0.0086$, $C = 0.5496$, $D_1(0) = -0.541$, $D_2(0) = 0.0653$, $k_1(0) = 0.05418$, $\dot{x}(0) = 0.0663$, and $\omega_1(0) = 1.0144$. As shown in Figures 2(a) and 2(c), the highest vibration amplitudes occur during the transient oscillations. This transient oscillatory behavior provides information to ensure that the system design constraints are not exceeded, even if the shear suspension system performs well during its steady-state behavior. Figure 2(b) shows the phase plane of the transient oscillatory motion on the time interval $0 \leq t \leq 31$ plotted by considering the following initial conditions of $x_0 = 0$ and $\dot{x}_0 = 0.0663$. It is clear from Figure 2(b) that the transient oscillations experience a fast increase in their amplitude values followed by a decrease when $t > 31$, as illustrated in Figure 2(c). When the system reaches its steady-state behavior, the system phase portrait, depicted in Figure 2(d), exhibits stable behavior about the steady-state equilibria condition.

We next investigate the influence of the transient solution on the dynamics response of (28) by introducing the percentage of overshoot which is defined as

$$\%\ \text{overshoot} = \left(\frac{x_{\text{tran}} - x_{\text{st}}}{x_{\text{st}}}\right) \times 100, \tag{30}$$

where x_{trans} and x_{st} represent the peak transient and steady-state amplitudes of the system, respectively, that can be estimated by setting to zero the time derivative of (23). Figure 3 shows the calculated system overshoot plotted against the system angular frequency, ω_f, by considering the following system parameter values: $\sigma_e = 0.497$, $F = 0.1$, $\nu = 0.01$, and $x_0 = 0$. As we can see from Figure 3, the influence of the transient solution on the system response is evident since the percentage of overshoot values is close to a 100% at the approximate frequency values of 0.1, 0.5, 1.5, and 2.

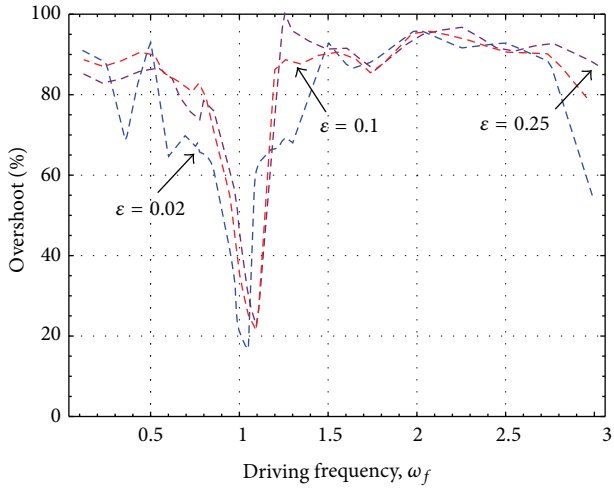

FIGURE 3: Percentage overshoot versus the driving frequency for parameter values of $\sigma_e = 0.497$, $F = 0.1$, $\nu = 0.01$, $x_0 = 0$, and $\varepsilon = 0.02$, 0.1, and 0.25.

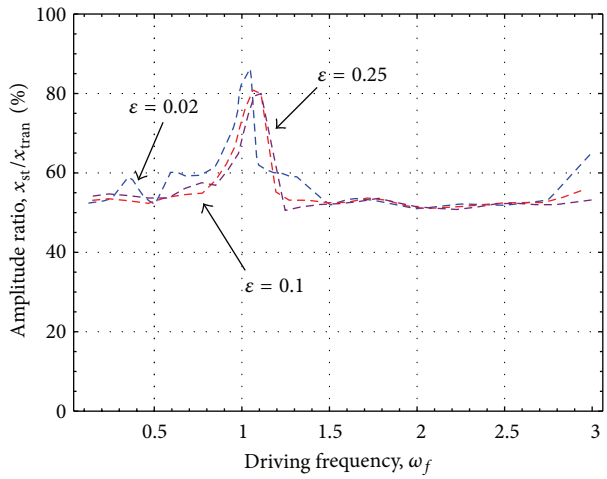

FIGURE 4: Transient and steady-state amplitude ratio (x_{tran}/x_{st}) versus the driving frequency. Here the parameter values are $\sigma_e = 0.497$, $F = 0.1$, $\nu = 0.01$, $x_0 = 0$, and $\varepsilon = 0.02$, 0.1, and 0.25.

Here the blue, the red, and the purple dashed lines were calculated by considering the nonlinear parameter values of $\varepsilon = 0.02$, 0.1, and 0.25, respectively. It is interesting to observe in Figure 3 the influence of the nonlinearity of the system in the overshoot qualitative and quantitative curves behavior. In fact, one can conclude from Figure 3 that the smallest percentage values of the overshoot occur with $\varepsilon = 0.02$ and near to the resonance frequency. Furthermore, the predicted overshoot curves oscillate about the value of 92% on the interval $1.5 \leq \omega_f \leq 2.7$ that corresponds to the region depicted in Figure 4 at which the ratio of the transient and the steady-state amplitudes has almost the constant value of 52%.

To examine damping effects on the system overshoot, we next use the parameter values of $\sigma_e = 0.497$, $F = 0.1$, $\varepsilon = 0.02$, and $x_0 = 0$ and consider the damping ratio values of $\nu = 0.01$, 0.05, and 0.1. The influence of the transient response on the peak overshoot values for the curve in which $\varepsilon = 0.02$, $\nu = 0.01$, $\omega_f = 0.5$ and 1.5 is illustrated in Figures 5(a) and 5(b). Figure 5(c) shows the percentage overshoot curves plotted against the driving frequency ω_f. As me can see from Figure 5(c) and for a damping value of $\nu = 0.1$, the overshoot values do not exceed 73%. It is also observed that for increasing damping values, the percentage of the system overshoot becomes smaller. Figures 5(d) and 5(e) illustrate, by using the Continuous Wavelet Transform, the influence of the transient and the driving frequencies on the nonlinear behavior of the system. It is evident from Figures 5(d) and 5(e) that at the beginning of the system motion, the transient frequency ω_1 influences the fast increase of the system oscillations. Then, its effects on the system non-linear motion decrease when the running time exceeds the value of $t \approx 200$. Based on these findings, it is concluded that transient amplitude values are bigger than those of the steady-state ones as showed in Figures 3 and 5. Therefore, if one wants to reduce the impact of the transient oscillations amplitudes, we need, when possible, a fast tuning of the system to its operating bandwidth frequency region which can be achieved by using suitable control algorithms.

4. Conclusions

In this paper, we have used elliptic functions to obtain the transient and the steady-state solutions of an asymmetric Duffing oscillator and studied its influence on the region of the primary resonance response. The theoretical predictions of our derived solution given by (23) are based on the assumption that the physical parameters $\omega_1(t)$, $D_1(t)$, $D_2(t)$, $k_1(t)$, and $b(t)$ are slowly varying as a function of time. To obtain computational tractable expressions to determine the aforementioned parameters, we have computed the average of the corresponding equations with respect to the complete elliptic integral of the first kind for the moduli k_1 and k_f. Then, we have used Fourier series and followed the harmonic balance method to balance the lowest harmonic terms. These steps plus the assumption that $0 < |k_1^2| < 1/2$ provide us with the time-dependent equations to determine the unknown parameters. The effect of the running time on the shapes of the amplitude-frequency response curves becomes evident during the study of the dynamical oscillator response with no linear stiffness term and with hardening characteristics. We have also shown that when the running time increases, the frequency range at which unstable motion occurs becomes smaller. Furthermore, we have obtained the percentage overshoot charts to address the influence of the nonlinear and damping terms on the transient and steady-state system responses when the system is suddenly switched on. We have found that when the nonlinearity is small, the percentage overshoot values becomes smaller at the overshoot bandwidth regions closer to the resonance frequency with increasing values of the steady-state and the transient amplitudes ratio. The usage of Continuous Wavelet Transform helps to identify the influence of the transient response signal on the system behaviour as time evolve.

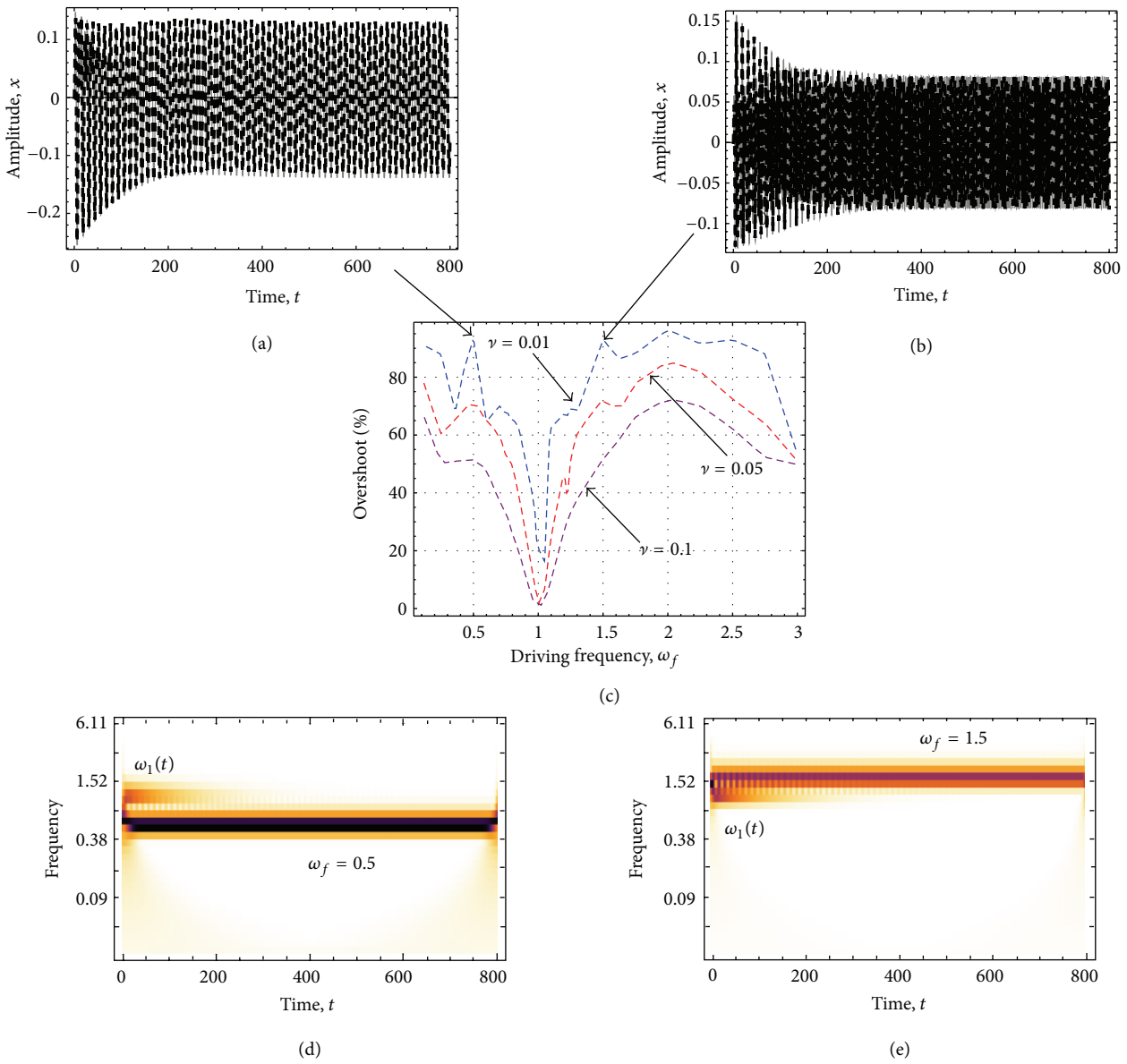

FIGURE 5: System nonlinear dynamic behavior for parameter values of $\sigma_e = 0.497$, $F = 0.1$, $\varepsilon = 0.02$, $x_0 = 0$. Here, (a) and (b) show the amplitude versus time response curves for which the solid black and the dashed black lines represent the numerical and the EBM solutions, respectively; (c) illustrates the percentage overshoot versus the driving frequency for damping values of $\nu = 0.01$, 0.05, and 0.1; (d) and (e) exhibit the influence of the transient and driving frequencies on the nonlinear system motion by using the Continuous Wavelet Transform.

We also found that by adding damping to the system, the percentage of overshoot in the system does not exceed, in the case of $\nu = 0.1$, 52% if the system is tuned into the overshoot bandwidth region of $0.5 \leq \omega_f \leq 1.5$.

Based on these findings, we can conclude that if one really wants to have a better understanding of the system dynamical behavior, transient oscillations amplitudes must be estimated to avoid undesirable system effects such as peak transient amplitude values that could violate design constraints or unstable system behavior when the excitation is suddenly switched on. In this case, the percentage overshoot charts could be used to identify the frequency bandwidth region at which the system can be tuned to have a reliable dynamical response.

Appendix

The terms I_j in (6) can be computed from

$$I_j \equiv \frac{1}{4K_j}\int_{\phi_j}^{4K_j+\phi_j} \mathrm{cn}_j^2 d\Psi_j = 1 - \frac{1}{k_j^2}\left(1 - \frac{E_j}{K_j}\right); \quad \Psi_j \equiv \omega_j t + \phi_j, \tag{A.1}$$

where E_j represents the complete elliptic integral of the second kind for the modulus k_j [20, 21].

The terms H_1, H_2, and H_3 in (9) are defined as

$$\begin{aligned} H_1 &= \frac{1}{\pi}\int_0^{2\pi} \mathrm{sn}u\mathrm{dn}u\sin\varphi d\varphi = \frac{1}{\pi}\int_0^{4K} \mathrm{sn}u^2\mathrm{dn}u^2\mathrm{d}u \\ &= \frac{4}{3k_f^2\pi}\left[\left(2k_f^2-1\right)E_f + K_f\left(1-k_f^2\right)\right], \\ H_2 &= \frac{1}{\pi}\int_0^{2\pi} \mathrm{cn}u\mathrm{dn}u\cos\varphi d\varphi = \frac{1}{\pi}\int_0^{4K} \mathrm{cn}u^2\mathrm{dn}u^2\mathrm{d}u \\ &= \frac{4}{3k_f^2\pi}\left[\left(1+k_f^2\right)E_f - K_f\left(1-k_f^2\right)\right], \\ H_3 &= \frac{1}{\pi}\int_0^{2\pi} \mathrm{sn}u\mathrm{cn}u^2\sin\varphi\mathrm{d}\varphi \\ &= \frac{1}{\pi}\int_0^{4K} \mathrm{sn}u^2\mathrm{cn}u^2\mathrm{dn}u\mathrm{d}u = \frac{1}{4}. \end{aligned} \tag{A.2}$$

Here $\varphi_j = \mathrm{am}(\omega_j t; k_j^2)$ is called the amplitude for Jacobi elliptic functions.

Acknowledgment

This work was partially funded by the Tecnológico de Monterrey, Campus Monterrey, through the Research Chairs in Nanotechnology and Intelligent Machines. Additional support was provided by the project FOMIX NL-2010-C30-145429.

References

[1] J. J. Stoker, *Non-Linear Vibrations in Mechanical and Electrical Systems*, Intersciense, New York, NY, USA, 1950.

[2] A. H. Nayfeh, "Resolving controversies in the application of the method of multiple scales and the generalized method of averaging," *Nonlinear Dynamics*, vol. 40, no. 1, pp. 61–102, 2005.

[3] H. Hu, "Exact solution of a quadratic nonlinear oscillator," *Journal of Sound and Vibration*, vol. 295, no. 1-2, pp. 450–457, 2006.

[4] M. Belhaq and F. Lakrad, "On the elliptic harmonic balance method for mixed parity non-linear oscillators," *Journal of Sound and Vibration*, vol. 233, no. 5, pp. 935–937, 2000.

[5] H. Tamura, "Exact solutions of the free vibration of a nonlinear system with a quadratic spring: expressions of the solution and trial methods for the Fourier coefficients," *The Japan Society of Mechanical Engineers International Journal*, vol. 33, no. 4, pp. 506–512, 1990.

[6] H. Hu, "Solution of a mixed parity nonlinear oscillator: harmonic balance," *Journal of Sound and Vibration*, vol. 299, no. 1-2, pp. 331–338, 2007.

[7] H. Cao, J. M. Seoane, and M. A. F. Sanjuán, "Symmetry-breaking analysis for the general Helmholtz-Duffing oscillator," *Chaos, Solitons & Fractals*, vol. 34, no. 2, pp. 197–212, 2007.

[8] A. Elías-Zúñiga, "Analytical solution of the damped Helmholtz-Duffing equation," *Applied Mathematics Letters*, vol. 25, no. 12, pp. 2349–2353, 2012.

[9] I. Kovacic, M. J. Brennan, and B. Lineton, "On the resonance response of an asymmetric Duffing oscillator," *International Journal of Non-Linear Mechanics*, vol. 43, no. 9, pp. 858–867, 2008.

[10] S. Jeyakumari, V. Chinnathambi, S. Rajasekar, and M. A. F. Sanjuan, "Vibrational resonance in an asymmetric duffing oscillator," *International Journal of Bifurcation and Chaos*, vol. 21, no. 1, pp. 275–286, 2011.

[11] J. J. Sinou, "Transient non-linear dynamic analysis of automotive disc brake squeal—on the need to consider both stability and non-linear analysis," *Mechanics Research Communications*, vol. 37, no. 1, pp. 96–105, 2010.

[12] R. J. Monroe and S. W. Shaw, "On the transient response of forced nonlinear oscillators," *Nonlinear Dynamics*, vol. 67, no. 4, pp. 2609–2619, 2012.

[13] R. J. Monroe and S. W. Shaw, "Nonlinear transient dynamics of pendulum torsional vibration absorbers—part I: theory," *Journal of Vibration and Acoustics*, vol. 135, no. 1, Article ID 011017, 10 pages, 2013.

[14] X. Dong, G. Chen, and L. Chen, "Controlling the uncertain Duffing oscillator," in *Proceedings of the 1st International Conference on Control of Oscillations and Chaos*, vol. 2, pp. 419–422, August 1997.

[15] S. Bowong, F. M. Moukam Kakmeni, and J. L. Dimi, "Chaos control in the uncertain Duffing oscillator," *Journal of Sound and Vibration*, vol. 292, no. 3-5, pp. 869–880, 2006.

[16] A. Elías-Zúniga, "Analysis of a beam-column system under varying axial forces of elliptic type: the exact solution of Lamé's equation," *International Journal of Solids and Structures*, vol. 41, no. 8, pp. 2155–2163, 2004.

[17] S. M. Sah and B. Mann, "Transition curves in a parametrically excited pendulum with a force of elliptic type," *Proceedings of the Royal Society of London. Series A*, vol. 468, no. 2148, pp. 3995–4007, 2012.

[18] A. Elías-Zúñiga, "A general solution of the Duffing equation," *Nonlinear Dynamics*, vol. 45, no. 3-4, pp. 227–235, 2006.

[19] V. T. Coppola and R. H. Rand, "Averaging using elliptic functions: approximation of limit cycles," *Acta Mechanica*, vol. 81, no. 3-4, pp. 125–142, 1990.

[20] P. F. Byrd and M. D. Friedman, *Handbook of Elliptic Integrals for Engineers and Physicists*, Springer, Berlin, Germany, 1954.

[21] A. Elías-Zuñiga, "On the elliptic balance method," *Mathematics and Mechanics of Solids*, vol. 8, pp. 263–269, 2003.

[22] A. Elías-Zúñiga, "Application of Jacobian elliptic functions to the analysis of the steady-state solution of the damped duffing equation with driving force of elliptic type," *Nonlinear Dynamics*, vol. 42, no. 2, pp. 175–184, 2005.

[23] R. E. Mickens, "A generalization of the method of harmonic balance," *Journal of Sound and Vibration*, vol. 111, no. 3, pp. 515–518, 1986.

[24] A. Elías-Zúñiga and M. F. Beatty, "Forced vibrations of a body supported by viscohyperelastic shear mountings," *Journal of Engineering Mathematics*, vol. 40, no. 4, pp. 333–353, 2001.